Solid-State NMR Investigation of the Selective Disruption of Lipid Membranes by Protegrin-1[†]

Rajeswari Mani,[‡] Jarrod J. Buffy,[‡] Alan J. Waring,[§] Robert I. Lehrer,[§] and Mei Hong*[,‡]

Department of Chemistry, Iowa State University, Ames, Iowa 50011, and Department of Medicine, University of California at Los Angeles School of Medicine, Los Angeles, California 90095

Received June 28, 2004; Revised Manuscript Received August 24, 2004

ABSTRACT: The interaction of a β-hairpin antimicrobial peptide, protegrin-1 (PG-1), with various lipid membranes is investigated by ^{31}P, ^{2}H, and ^{13}C solid-state NMR. Mixed lipid bilayers containing anionic lipids and cholesterol are used to mimic the bacterial and mammalian cell membranes, respectively. ^{31}P and ^{2}H spectra of macroscopically oriented samples show that PG-1 induces the formation of an isotropic phase in anionic bilayers containing phosphatidylglycerol. Two-dimensional ^{31}P exchange experiments indicate that these isotropic lipids are significantly separate from the residual oriented lamellar bilayers, ruling out toroidal pores as the cause for the isotropic signal. ^{1}H spin diffusion experiments show that PG-1 is not exclusively bound to the isotropic phase but is also present in the residual oriented lamellar bilayers. This dynamic and morphological heterogeneity of the anionic membranes induced by PG-1 is supported by the fact that ^{13}C T_2 relaxation times measured under cross polarization and direct polarization conditions differ significantly. In contrast to the anionic membrane, the zwitterionic phosphatidylcholine (PC) membrane does not form an isotropic phase in the presence of PG-1 but shows significant orientational disorder. The addition of cholesterol to the PC bilayer significantly reduces this orientational disorder. The ^{13}C T_2 relaxation times of the PC lipids in the presence of both cholesterol and PG-1 suggest that the peptide may decrease the dynamic heterogeneity of the cholesterol-containing membrane. The observed selective interaction of PG-1 with different lipid membranes is consistent with its biological function and may be caused by its strong cationic and amphipathic structure.

Antimicrobial peptides are potent microbicidal molecules produced by many plants, amphibians, mammals, and other organisms (*1*, *2*). Most of these peptides kill microbial cells by disrupting their cell membranes. One of the most intriguing aspects of antimicrobial activity of peptides is their selective disruption of microbial cell membranes but relatively moderate toxicity toward host cell membranes. Many studies on antimicrobial peptides have been carried out in an effort to elucidate the cause for this selectivity. One hypothesis is that the highly anionic lipids (~30 mol %) (*3*, *4*) in the cytoplasmic membranes of bacterial and fungal cells facilitate antimicrobial action by electrostatically attracting these cationic peptides to the membrane. In contrast, the lack of negative charges in the eukaryotic membrane of higher organisms combined with the high level of cholesterol (~50 mol %) (*5*, *6*) may reduce the extent of binding and counter the effects of these peptides on the membrane. Indeed, charge- and cholesterol-dependent antimicrobial activity has been observed for a number of peptides such as magainins (*7*, *8*), gramicidin S (*9*), tachyplesin (*10*), and cecropins (*11*), using both activity assays and biophysical measurements such as fluorescence spectroscopy, NMR, and differential scanning calorimetry.

Protegrin-1 (PG-1)[1] is an 18-residue β-hairpin peptide found in porcine leukocytes (*12*). The peptide contains two disulfide bonds from its four Cys residues. These disulfide bonds not only hold the two strands of the β-hairpin together (*13*, *14*) but also are crucial to antimicrobial activity (*15*, *16*). Like many antimicrobial peptides, PG-1 is highly cationic, with six Arg residues at the N- and C-termini and at the β-turn. This makes PG-1 an amphipathic molecule with a significant hydrophobic patch at the center. PG-1 kills Gram-positive bacteria, Gram-negative bacteria, and fungi (*15*, *17*, *18*), and has moderate antiviral activity against HIV-1 (*19*). The minimal inhibitory concentrations (MICs) of PG-1 against various bacteria and fungi range from 0.1 to 3 μM (*17*, *18*), while the PG-1 concentration that causes 50% hemolysis (EC_{50}) is ~80 μM (*18*). Thus, PG-1 selects bacterial membranes over eukaryotic membranes by 1−2 orders of magnitude.

Our recent solid-state NMR investigations showed that PG-1 interacts with phosphatidylcholine (PC) lipids in a concentration- and chain length-dependent manner (*20*). Above 3% peptide, PG-1 causes strong orientational disorder

[†] This work is supported by National Institutes of Health Grant GM-066976 to M.H. and Grants AI-22839 and AI-37945 to A.J.W. and R.I.L.

* To whom correspondence should be addressed: Department of Chemistry, Iowa State University, Ames, IA 50011. Telephone: (515) 294-3521. Fax: (515) 294-0105. E-mail: mhong@iastate.edu.

[‡] Iowa State University.

[§] University of California at Los Angeles School of Medicine.

[1] Abbreviations: PG-1, protegrin-1; NMR, nuclear magnetic resonance; POPC, 1-palmitoyl-2-oleoyl-*sn*-glycero-3-phosphatidylcholine; POPG, 1-palmitoyl-2-oleoyl-*sn*-glycero-3-phosphatidylglycerol; Chol, cholesterol; MAS, magic angle spinning; CP, cross polarization; DP, direct polarization; CSA, chemical shift anisotropy.

10.1021/bi048650t CCC: $27.50
Published on Web 10/05/2004

of POPC membranes. Motionally averaged chemical shift anisotropies and dipolar couplings indicate that PG-1 is uniaxially mobile in DLPC bilayers, which have 12 carbons in the acyl chains, but immobilized in POPC bilayers, which have 16−18 carbons in the acyl chains (*21*). In DLPC bilayers, PG-1 inserts fully into the membrane (*22*) with its β-strand axis tilted by ~55° from the bilayer normal (*20*).

While these NMR studies provided useful insight into the membrane requirement for PG-1 insertion and the depth and orientation of the inserted peptide, they did not address the origin for the selective membrane disruption by PG-1. On the other hand, measurement of the activities of PG-1 toward various organisms (*16*, *18*) did not give insight into the molecular mechanism of interaction of PG-1 with lipids and cholesterol.

To bridge the gap between the activity studies and the structural studies of PG-1 and better understand the origin of PG-1's membrane selectivity, we have undertaken an NMR investigation of the interaction of PG-1 with membranes of varying lipid compositions. Solid-state NMR is a powerful spectroscopic tool for determining the structure and dynamics of membranes in the presence of peptides. ^{31}P, ^{13}C, and ^{2}H NMR probes both the headgroup and the hydrophobic interior of lipid bilayers. Information about the dynamic and static disorder and the morphology of the lipid membrane can be readily obtained from the anisotropic line shapes of the NMR spectra. Specifically, here we investigate how the addition of anionic phosphatidylglycerol lipids and neutral cholesterol molecules to POPC bilayers affects PG-1's interaction with the membrane. By using macroscopically oriented membranes, which have much better resolved ^{31}P peaks than unoriented powder samples, we readily identify and distinguish lipid domains with different mobilities and morphologies. ^{2}H NMR of chain-perdeuterated lipids provides complementary information about the dynamic disorder of the hydrophobic core of the bilayer that may be induced by PG-1. Qualitative information about the partition of PG-1 into different lipid morphologies is obtained using ^{1}H spin diffusion. Finally, we investigate the dynamic heterogeneity of the membranes in the absence and presence of PG-1 using differential ^{13}C T_2 relaxation times between cross polarization (CP) and direct polarization (DP) conditions.

EXPERIMENTAL PROCEDURES

Materials. All lipids were purchased from Avanti Polar Lipids (Alabaster, AL) and used without further purification. These include 1-palmitoyl-2-oleoyl-*sn*-glycero-3-phosphatidylcholine (POPC), 1-palmitoyl-d_{31}-2-oleoyl-*sn*-glycero-3-phosphatidylcholine (POPC-d_{31}), 1-palmitoyl-2-oleoyl-*sn*-glycero-3-phosphatidylglycerol (POPG), 1-palmitoyl-d_{31}-2-oleoyl-*sn*-glycero-3-phosphatidylglycerol (POPG-d_{31}) (custom synthesis), and cholesterol. PG-1 was synthesized according to previously published procedures (*20*). Trifluoroethanol (TFE), chloroform, and cyclohexane were obtained from Aldrich Chemicals (Milwaukee, WI). Glass cover slides ~80 μm in thickness were obtained from Marienfeld Laboratory Glassware and cut into 6 mm × 12 mm rectangles.

Sample Preparation. Glass plate-oriented membrane mixtures were prepared using a naphthalene-incorporated procedure described recently (*23*). The peptide was dissolved in TFE and mixed with a chloroform solution of the desired lipids. The mixture was dried under a stream of N_2 gas, and the dried film was redissolved in a 2:1 chloroform/TFE mixture containing a 5-fold excess of naphthalene with respect to the lipids. The solution was deposited on 20 glass plates at a surface concentration of 0.01−0.02 mg/mm^2, air-dried for 2 h, and then vacuum-dried for 5 h to remove all solvents and naphthalene. Approximately 1 μL of water was added directly to each glass plate, and then the sample was hydrated indirectly at a relative humidity of 95% over a saturated solution of Na_2HPO_4 for 2−3 days at room temperature. The glass plates were stacked, wrapped in Parafilm, and sealed in a polyethylene bag to prevent dehydration.

Unoriented membrane samples for MAS experiments were prepared by codissolving PG-1 and the lipids in TFE and chloroform solutions to achieve the desired peptide:lipid molar ratio (P:L). Approximately 20−40 mg of lipid was dissolved in ~4 mL of chloroform, and PG-1 was dissolved in ~1 mL of TFE. The combined solution was dried under a stream of nitrogen gas, and the resulting film was redissolved in ~4 mL of cyclohexane, frozen in liquid nitrogen, and lyophilized. The resulting dry peptide/lipid mixed powder was packed into 4 mm rotors and hydrated to 35% water by weight. A Teflon spacer was used to center the sample in the rotor to reduce radio frequency field inhomogeneity.

Solid-State NMR. NMR experiments were carried out on a Bruker Avance (Karlsruhe, Germany) DSX-400 spectrometer operating at resonance frequencies of 162.12 MHz for ^{31}P, 100.72 MHz for ^{13}C, and 61.48 MHz for ^{2}H. A static double-resonance probe equipped with a custom-designed rectangular coil was used for oriented-membrane experiments, while MAS experiments were conducted on a 4 mm double-resonance probe with spinning speeds of 2.5−4.0 kHz. The ^{31}P chemical shift was referenced externally to 85% phosphoric acid at 0 ppm, and the ^{13}C chemical shift was referenced to the α-glycine carbonyl signal at 176.4 ppm on the TMS scale. The ^{31}P spectra of oriented samples typically required 1000 scans of signal averaging, while ~4000 scans were coadded for the ^{13}C MAS spectra under both CP and DP conditions. For oriented membrane samples tilted with the alignment axis at 90° from B_0, the ^{31}P chemical shift was corrected for susceptibility effects (*24*). This was done by comparing the ^{1}H chemical shift of water in a glass plate-oriented membrane sample at the 0° and 90° orientations. The 90° aligned sample exhibited an upfield shift of 4.8 ppm compared to the 0° aligned sample, while a control sample of pure water in a cylindrical tube showed no difference in chemical shift between the two orientations. Thus, the 90°-aligned ^{31}P spectra were corrected by adding 4.8 ppm to the nominal frequency. The corrected spectra show the same lipid 90° frequencies between the 0° and 90° alignment directions, as expected.

^{2}H spectra were acquired with the quadrupole echo sequence with a recycle delay of 0.5 s. ^{31}P experiments were carried out using a recycle delay of 2 s. Typical pulse lengths were 5 μs for ^{31}P and ^{1}H. ^{13}C T_2 relaxation times were measured using a Hahn echo sequence ($\tau-180°-\tau$) following either a ^{13}C 90° excitation pulse (direct polarization) or a ^{1}H−^{13}C cross polarization (CP) step. The Hahn echo delay τ ranged from 1 to 9 ms and is set to be an integer multiple of the rotor period. To remove the offset dependence of T_2

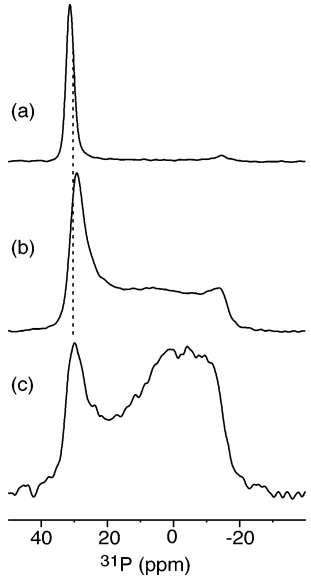

FIGURE 1: ^{31}P spectra of oriented POPC lipids with varying molar concentrations of PG-1: (a) 0%, (b) 1.3%, and (c) 4%. The control spectrum (a) shows nearly vanishing powder intensity, while the presence of PG-1 increases the disorder significantly.

relaxation, the 180° ^{13}C pulse was phase-cycled with respect to the excitation pulse or the ^{13}C spin lock pulse using the EXOYCYCLE scheme (*25*). The decay of the echo intensities as a function of 2τ was fit to a single-exponential decay to yield the T_2 value.

The ^{31}P-detected ^{1}H spin diffusion experiments were carried out using the ^{1}H 90°$-\tau-^1$H 180°$-\tau-^1$H 90°$-t_{mix}-^1$H 90°$-(^1$H,^{31}P) CP$-^{31}$P FID pulse sequence (see Figure 8a). This is the one-dimensional (1D) version of the two-dimensional (2D) spin diffusion experiments we introduced recently (*26*). The ^{1}H echo period (2τ) acts as a T_2 filter to select the ^{1}H magnetization of the mobile lipids while suppressing the rigid peptide magnetization. The value of 2τ ranged from 0 to 20 μs. The mixing time (t_{mix}) during which ^{1}H spin diffusion occurs ranged from 5 to 100 ms.

RESULTS

Interaction of PG-1 with Zwitterionic and Anionic Membranes. Figure 1 shows the ^{31}P spectra of zwitterionic POPC bilayers with varying concentrations of PG-1. Unless otherwise stated, the spectra were acquired with the glass plate normal parallel to the external magnetic field B_0. In the absence of the peptide (Figure 1a), the ^{31}P spectrum shows a dominant 0° frequency peak at 30 ppm with nearly vanishing intensity elsewhere, indicating that the lipids are well-aligned. Such control spectra generally exhibit percentages of alignment of 75−85%, as shown in Figure 5, attesting to the high degree of orientational order of the membrane in the absence of the peptide. At 1.3% PG-1, the intensities between −15 and 20 ppm grow noticeably, indicating the onset of orientational disorder. At 4% PG-1, the intensities from −15 to 20 ppm dominate the spectrum, indicating that the majority of the membrane has become unoriented. This broad line shape deviates significantly from the powder pattern of a randomly oriented sample, suggesting that in addition to the orientational disorder, the lipid headgroup conformation may have changed or the lipids may undergo intermediate time scale motion due to PG-1 binding.

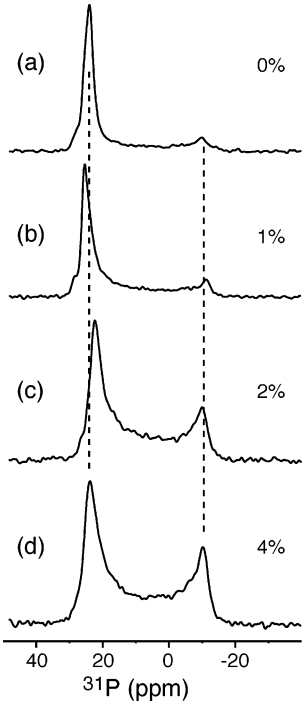

FIGURE 2: ^{31}P spectra of an oriented POPC/cholesterol (1.2:1 molar ratio) membrane with varying concentrations of PG-1: (a) 0%, (b) 1%, (c) 2%, and (d) 4%.

To test whether cholesterol, which is present at ∼50 mol % in mammalian cell membranes but absent in bacterial membranes, protects the lipid bilayer against PG-1, we prepared POPC/cholesterol (Chol) bilayers at a molar ratio of 1.2:1 and probed the effect of PG-1 on the orientational order of the mixed membrane. Figure 2 shows the ^{31}P spectra of POPC/Chol bilayers with 0−4% PG-1 (calculated with respect to POPC). In the absence of PG-1, the bilayers are well-aligned, exhibiting a dominant 0° ^{31}P peak at 25 ppm and negligible 90° intensity. The addition of PG-1 moderately increases the disorder. The intensities away from the 0° peak grow less compared to the POPC membrane. At 4% PG-1, the disorder is manifested mainly as a 90° frequency peak at −10 ppm while the intensity near the isotropic shift (1 ppm) is much weaker than the corresponding POPC spectrum (Figure 2d).

Anionic POPC/POPG (3:1 molar ratio) bilayers were prepared to mimic the bacterial cytoplasmic membrane. The ^{31}P spectra of POPC/POPG bilayers with and without PG-1 are shown in Figure 3. In addition to the general increase in powder intensities similar to those seen for the zwitterionic membranes, a distinct peak at 1.5 ppm grew with an increase in the PG-1 concentration. This peak is near the ^{31}P isotropic chemical shift and has a full width half-maximum of 1.6 kHz (∼10 ppm). This isotropic peak could originate from small lipid vesicles or micelles that undergo isotropic tumbling and lateral diffusion on time scales moderately faster than the inverse of the ^{31}P chemical shift anisotropy (CSA). Another possibility is the formation of cubic-phase lipids (*27*); however, given the large line width of the isotropic peak and the order required for cubic-phase lipids, this is a less likely scenario (*9*, *28*). The third possibility is toroidal pore defects within the lamellar bilayer, where the lateral diffusion of the pore-lining lipids over the curved surface reduces the ^{31}P CSA. In this latter case, since the

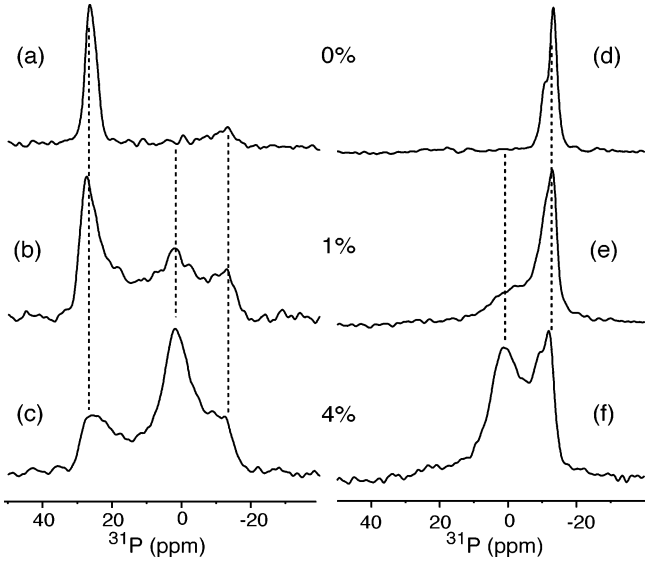

FIGURE 3: ^{31}P spectra of oriented POPC/POPG (3:1 molar ratio) lipids with (a and d) 0%, (b and e) 1%, and (c and f) 4% PG-1. The alignment axis is alternately parallel (a−c) and perpendicular (d−f) to the external magnetic field. The isotropic peak in spectra c and f resonates at 1.5 ppm.

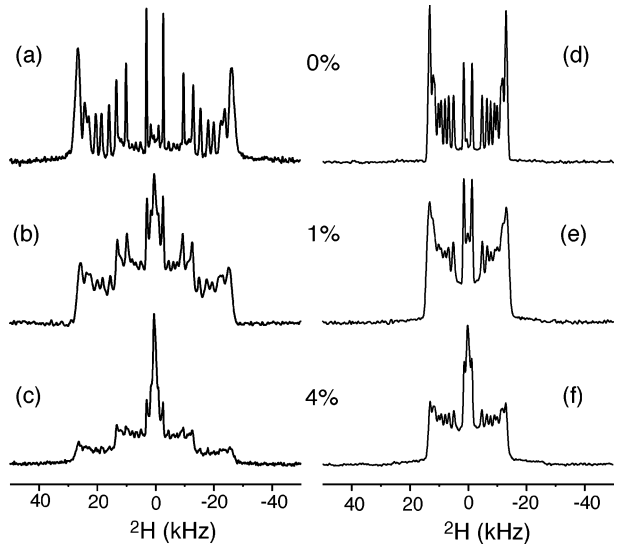

FIGURE 4: ^{2}H spectra of oriented d_{31}-POPC/POPG lipids with varying amounts of PG-1: (a and d) 0%, (b and e) 1%, and (c and f) 4%. The alignment axis is alternately parallel (a−c) and perpendicular (d−f) to the external magnetic field.

pore geometry is not spherical, the ^{31}P peak should be close to but not at the isotropic frequency.

To confirm that the 1.5 ppm peak in the POPC/POPG spectrum with 4% PG-1 does not have residual anisotropy, we measured the ^{31}P spectra of the same samples rotated by 90° so that the glass plate normal is perpendicular to B_0. The spectra (Figure 3d−f) show the same chemical shift of 1.5 ppm for the central peak, unchanged from the 0°-aligned spectra. Therefore, the central peak cannot result from lipids in nonspherical toroidal pores but most likely come from small vesicles or micelles as a result of fragmentation of the bilayer by PG-1.

^{2}H spectra of the *sn*-2 chain-perdeuterated POPC in the POPC/POPG bilayers provide further information about the nature of disorder induced by PG-1. Figure 4a−c shows the ^{2}H spectra acquired at the 0° alignment direction. In the absence of PG-1, a characteristic symmetric spectrum with multiple splittings was obtained, where the individual splittings reflect the dynamic order parameters, S_{CH}, of the CD_2 and CD_3 groups along the *sn*-2 chain (*26*, *29*, *30*). The more rigid methylene groups at the top of the acyl chain near the glycerol backbone have larger splittings, while the more mobile groups at the end of the acyl chain have smaller quadrupolar couplings. Figure 4a shows a maximum splitting of 53 kHz and a minimum of 5.8 kHz, corresponding to S_{CH} values of 0.21 and 0.02, respectively, consistent with the known C−H order parameters of liquid-crystalline bilayers (*30*). Upon addition of PG-1, the spectral resolution significantly worsened and the relative intensity of the small couplings in the center of the spectra increased; moreover, a zero-frequency peak grew to dominate the spectrum. These indicate that PG-1 not only increases the orientational disorder of the membrane but also promotes the formation of isotropic lipids, which are fully consistent with the ^{31}P data. There is no significant overall reduction of the C−H order parameters for the chain methylene groups, as the quadrupolar couplings remain similar to the control spectrum. To confirm this, we rotated the samples by 90° from B_0 and measured the ^{2}H spectra again (Figure 4d−f). When the glass plate normal is perpendicular to B_0, the spectral maximum of a perfectly aligned sample occurs when $P_2(\cos 90)\Delta\nu_Q = -0.5\Delta\nu_Q$, which coincides with the spectral maximum for a randomly oriented sample. Thus, at the 90° alignment direction, only changes of the motional order parameters, but not orientational distribution, can affect the ^{2}H quadrupolar coupling. Figure 4d−f shows that PG-1 does not alter the sizes of the individual splittings but only broadens the lines. Thus, PG-1 influences the orientation distribution but not the chain dynamics of the bilayer. The preservation of the C−H order parameters by PG-1 is the same as that observed on a POPC membrane without POPG (*20*), but differs from that of colicin Ia channel domain and ovispirin, which reduced the acyl chain order parameters, indicating membrane thinning (*29*, *31*).

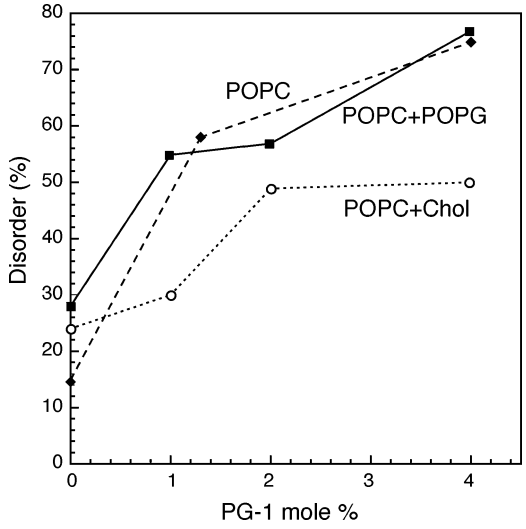

FIGURE 5: Membrane disorder as a function of PG-1 molar concentration for POPC (◆), POPC/POPG (■), and POPC/Chol (○) bilayers.

Figure 5 compares the disorder of the three different membranes as a function of PG-1 concentration. The disorder was calculated as the integrated intensity of the unoriented

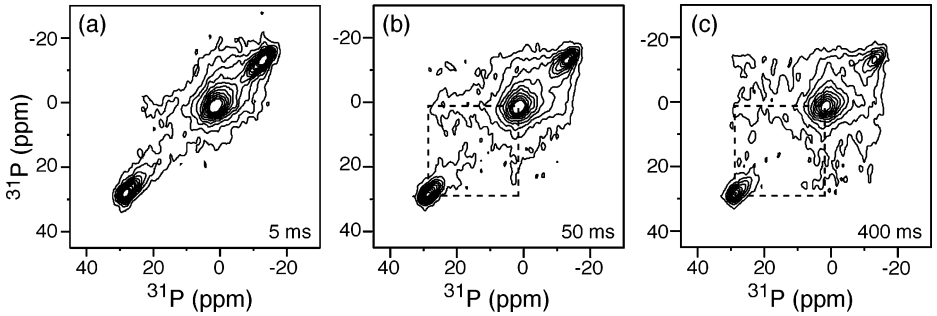

FIGURE 6: 2D ^{31}P exchange spectra of oriented POPC/POPG membranes with 4% PG-1. The exchange mixing times are (a) 5, (b) 50, and (c) 400 ms. Dashed lines guide the eye for the expected cross-peak positions between the 0° and isotropic peaks.

region of the ^{31}P spectra, defined to be 75% of the total chemical shift range starting from the upfield 90° peak, over the total intensity of the spectra. The POPC/POPG membrane and POPC membrane exhibit similarly high disorder in the presence of PG-1, while the POPC/Chol membrane shows the least disorder.

Structure of the POPC/POPG Membrane in the Presence of PG-1. To further elucidate if the isotropic lipids in POPC/POPG membranes are spatially separate from or a part of the residual lamellar bilayer, we conducted 2D ^{31}P exchange experiments. Lipids undergo lateral diffusion with diffusion coefficients of $10^{-7}-10^{-8}$ cm^2/s (*32*, *33*). If the isotropic lipids are contiguous with the residual oriented lipids, and if a typical radius of curvature of ~ 1 μm is assumed for the membrane, then the laterally induced lipid reorientation should change the ^{31}P frequency on time scales of 10−100 ms. This should give rise to cross-peaks in the 2D exchange spectra. Figure 6 displays the 2D ^{31}P spectra of the POPC/POPG/4% PG-1 sample acquired with mixing times of 5, 50, and 400 ms. At 5 ms, only diagonal intensities are observed, including the prominent 0°, 90°, and isotropic peaks. Increasing the mixing time produced only weak cross-peaks between the 0° peak and the isotropic peak despite their high diagonal intensities. This strongly suggests that the isotropic lipids reside in separate domains from the residual lamellar bilayer. Therefore, it is unlikely for the isotropic peak to reflect toroidal pores or other membrane defects within the oriented bilayer.

Since the isotropic peak in the POPC/POPG spectra is caused by PG-1, one may expect the peptide to be preferentially associated with the isotropic domain and the residual oriented lipids to be free of the peptide. To test this hypothesis, we conducted ^{31}P-detected 1D ^{1}H spin diffusion experiments using oriented d_{31}-POPC/d_{31}-POPG bilayers containing 4% PG-1. The pulse sequence of the experiment is shown in Figure 8a. A short ^{1}H T_2 filter first suppresses the ^{1}H magnetization of the rigid peptide while retaining the magnetization of the mobile lipid. A ^{1}H mixing time then allows the remaining lipid ^{1}H magnetization to be transferred to the peptide. After cross polarization from ^{1}H to ^{31}P, spin diffusion from the lipid to the peptide is manifested as a reduction in the ^{31}P intensity of the corresponding lipid domain. If the peptide is solely bound to the isotropic domain but absent in the residual oriented lamellar phase, then one would expect the isotropic ^{31}P peak to be reduced more than the 0° peak.

For the experiment to work, it is crucial for the number of lipid protons that participate in spin diffusion to be small and to be close to the ^{31}P nucleus. Comparison of 1D ^{1}H and 2D ^{1}H−^{31}P correlation MAS spectra of an unoriented POPC/POPG/PG-1 membrane showed that, after a 4 ms ^{1}H−^{31}P CP contact time, only the glycerol backbone and headgroup protons contribute to the ^{31}P magnetization (Figure 7). The static oriented experiments were conducted with a 2 ms CP; thus, the ^{1}H spin diffusion source should be even more selective and likely excludes the γ-proton and G1 proton. A second consideration is that if the acyl chain protons also transfer their magnetization to the peptide (*26*), then this alternative pathway would inhibit the desired magnetization transfer from the glycerol and headgroup protons. Thus, we used *sn*-2 chain-perdeuterated POPC and POPG lipids to inhibit the chain to peptide transfer. Double-chain perdeuteration is not commercially available for POPC and POPG lipids. The remaining protons in the oleoyl chain should not dilute the backbone magnetization transfer much,

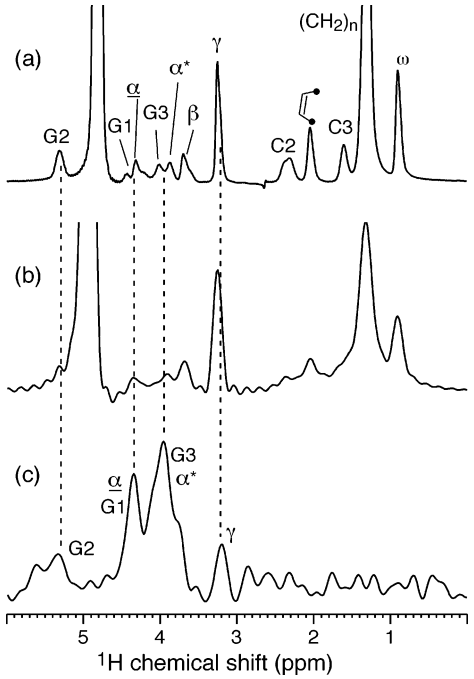

FIGURE 7: (a) 1D ^{1}H MAS spectrum of POPC/POPG without PG-1. Asterisks and underlines indicate the POPG and POPC sites, respectively, while the other assignments are the same for the two lipids (*50*). (b) ^{1}H MAS spectrum of POPC/POPG membranes with 4% PG-1. Note the line broadening caused by the peptide. (c) ^{1}H cross section of a ^{1}H−^{31}P 2D correlation spectrum acquired with a CP contact time of 4 ms. The headgroup and glycerol protons are selected because of their proximity to ^{31}P.

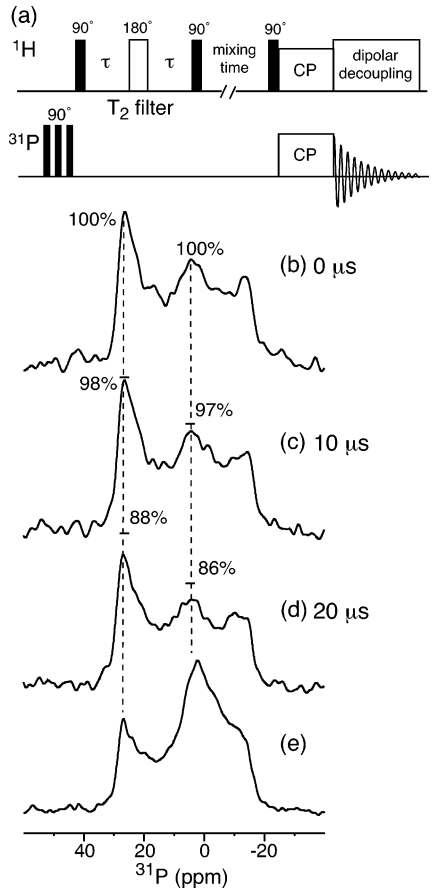

FIGURE 8: (a) Pulse sequence for the 1D ^{31}P-detected ^{1}H spin diffusion experiment. (b−d) ^{31}P spectra of the glass plate-oriented d_{31}-POPC/d_{31}-POPG/4% PG-1 membrane after ^{1}H spin diffusion. A ^{1}H T_2 filter (2τ) of (b) 0, (c) 10, and (d) 20 μs was used. The spin diffusion mixing time was 100 ms. (e) ^{31}P DP spectrum after the spin diffusion experiment showing a reproducible isotropic peak.

since the unsaturated chain is much more mobile than the glycerol backbone, making ^{1}H spin diffusion inefficient.

Figure 8b−d shows the ^{31}P spectra of the glass plate-aligned d_{31}-POPC/d_{31}-POPG membrane containing 4% PG-1. A ^{1}H spin diffusion mixing time of 100 ms and ^{1}H T_2 filter times (2τ) of 0, 10, and 20 μs were used. The ^{1}H−^{31}P contact time was 2 ms. In all three spectra, the intensity of the isotropic peak (dashed line) is reduced compared to that of the DP spectrum (Figure 8e) due to inefficient CP but still clearly visible. With an increase in ^{1}H T_2 filter time, both the isotropic and the 0° peak intensities decreased to similar extents. With a 20 μs ^{1}H T_2 filter, the 0° and isotropic peaks decreased to 87 ± 5%. Varying the spin diffusion mixing time and the ^{1}H−^{31}P contact time did not change this trend. The similar reduction of the oriented and isotropic peaks indicates that PG-1 is not exclusively bound to the isotropic domain but is also present in the residual oriented bilayers.

Dynamic Heterogeneity of the Mixed Membranes in the Presence of PG-1. To determine the degree of dynamic heterogeneity of the membranes in the presence of PG-1, we compared the ^{13}C T_2 relaxation times under CP and DP conditions. CP preferentially selects the signals of the rigid component due to its requirement for dipolar coupling, while the DP experiment preferentially detects the mobile components. If the membrane dynamics is uniform, then no difference is expected between the $T_{2,CP}$ and $T_{2,DP}$ values. This would yield a T_2 ratio of 1. Reduction of $T_{2,CP}/T_{2,DP}$ from unity indicates that the bilayers are dynamically heterogeneous.

Figure 9a shows the ^{13}C DP spectrum of a POPC/POPG membrane where the POPC ^{13}C assignment is indicated. The POPC ^{13}C T_2 values under CP and DP are shown in Figure 9b. In general, the T_2 values are shorter in the presence of the peptide than in its absence. This means that peptide binding causes lipid motions that are slower than the fast uniaxial rotational diffusion of the pure lamellar lipids. The DP experiment gives longer T_2 values than the CP experiment for both samples, but the difference is more pronounced for the PG-1-bound sample. As a result, the $T_{2,CP}/T_{2,DP}$ ratio decreased upon PG-1 binding (Figure 9c). Thus, the POPC/POPG bilayer becomes more heterogeneous in the presence of PG-1. A control experiment on a pure POPC bilayer without the peptide shows near-unity T_2 ratios for most sites, indicating homogeneous dynamics, which is expected for the one-component system (*21*).

Similar experiments were carried out on the POPC/Chol membrane. The T_2 values of the assigned POPC carbons (Figure 10a) with and without PG-1 are shown in Figure 10b. Noticeably, the CP and DP T_2 difference for each sample is now larger than the peptide-induced difference between two samples. Specifically, the $T_{2,CP}/T_{2,DP}$ ratios of the peptide-absent membrane are already significantly smaller than 1, indicating that cholesterol increases the membrane heterogeneity substantially (Figure 10a). The fact that the $T_{2,CP}$ and $T_{2,DP}$ values are both shorter than those of the POPC/POPG bilayer indicates that the cholesterol-containing membrane has slower motions than the POPC/POPG bilayer. This is consistent with the known condensing effect of cholesterol on biological membranes and the complex phase diagram of cholesterol-containing membranes (*34*−*36*).

The addition of PG-1 decreased $T_{2,DP}$ more than $T_{2,CP}$ so that the T_2 ratios of the PG-1-bound POPC/Chol membrane are higher than those of the peptide-absent membrane. Thus, it appears that PG-1 makes the POPC/Chol membrane more homogeneous, possibly by interacting with the POPC-rich region of the membrane and inducing slower-time scale motions in these lipids.

DISCUSSION

In this work, we examine the origin of membrane selectivity of PG-1, a representative β-sheet antimicrobial peptide that destroys bacterial and fungal cells with a higher efficiency (1−2 orders of magnitude) than erythrocytes (*18*). We test the hypothesis that the high percentage of anionic lipids in bacterial and fungal cytoplasmic membranes facilitates PG-1's disruption of membrane structure while the cholesterol in mammalian membranes attenuates its lytic activity. While other hypotheses such as the presence of outer membrane lipopolysaccharides (LPS) (*37*) and the propensity of lipids to form nonlamellar structures (*27*) have also been proposed to contribute to antimicrobial selectivity, these are less general mechanisms. LPS is present only in Gram-negative bacteria, and nonlamellar phases are formed only by certain lipids. We use POPC/cholesterol (1.2:1) bilayers to mimic the mammalian plasma membranes and POPC/POPG (3:1) bilayers to mimic the bacterial cytoplasmic membranes, and monitor how these composition changes

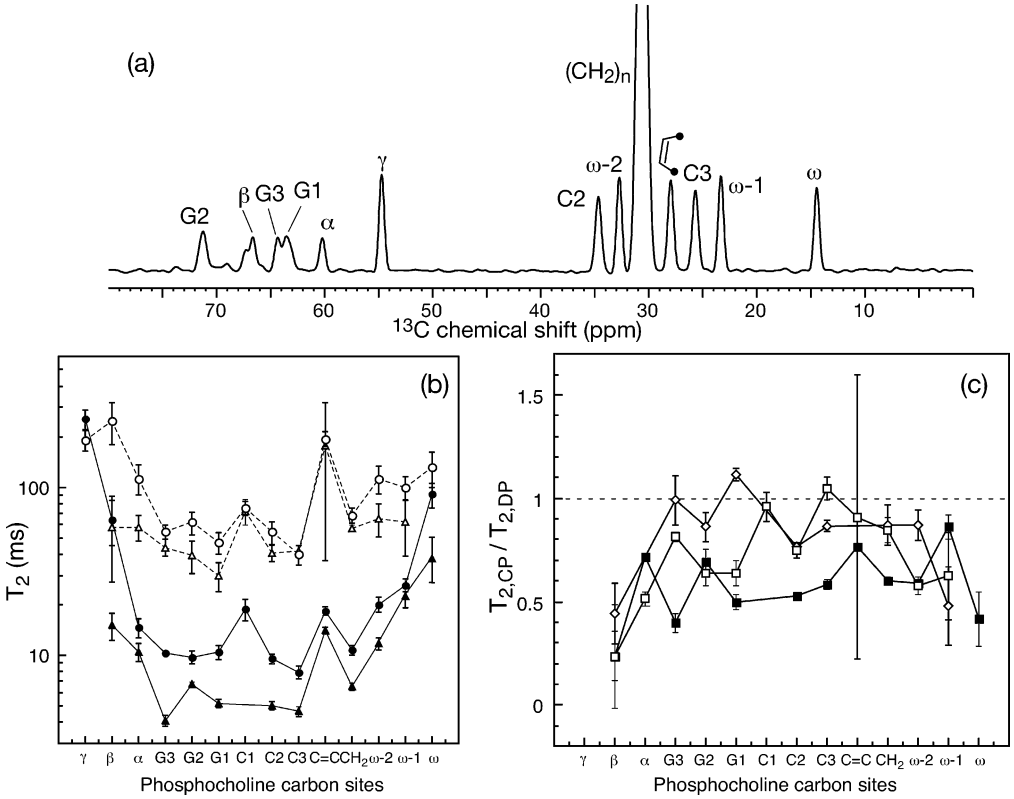

FIGURE 9: (a) ^{13}C DP-MAS spectrum of a POPC/POPG membrane without PG-1. The POPC ^{13}C assignment is indicated (*51*). (b) ^{13}C T_2 relaxation times of POPC in POPC/POPG membranes in the absence (empty symbols) and presence (filled symbols) of PG-1: (circles) DP and (triangles) CP. (c) Ratio of CP and DP T_2 values for the POPC control (◇), the POPC/POPG membrane without PG-1 (□), and the POPC/POPG membrane with 4% PG-1 (■).

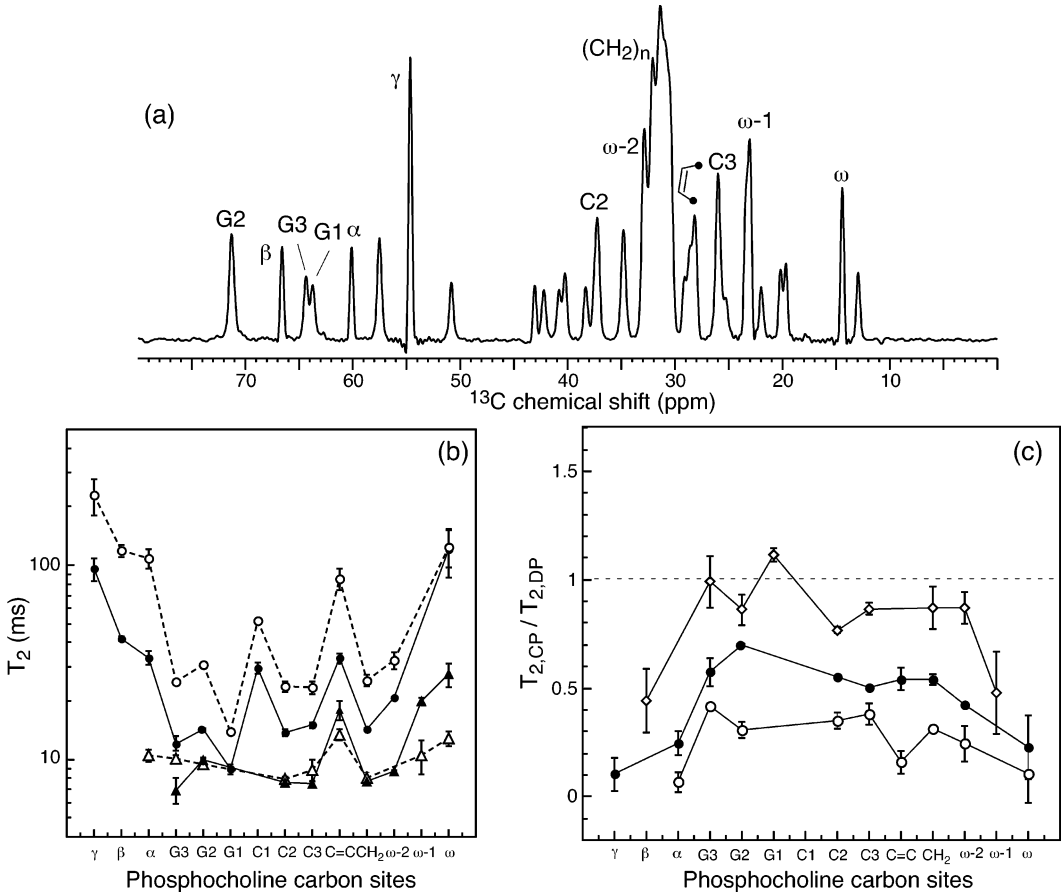

FIGURE 10: (a) ^{13}C DP-MAS spectrum of a POPC/Chol membrane, indicating the POPC ^{13}C assignment (*51*). (b) ^{13}C T_2 relaxation times of POPC in the POPC/Chol membrane in the absence (empty symbols) and presence (filled symbols) of PG-1: (circles) DP and (triangles) CP. (c) Ratio of CP and DP T_2 values for the POPC control (◇), the POPC/Chol membrane without PG-1 (○), and the POPC/Chol membrane with 4% PG-1 (●).

affect the interaction between PG-1 and the lipid bilayer. Studies using model lipid bilayers have provided useful insight into the mechanism of action of peptides (*38*, *39*).

The ^{31}P spectra of the oriented samples show unambiguously that PG-1 causes much disorder already in simple POPC bilayers, but this disorder is made significantly worse with the addition of POPG, since a new isotropic phase is created. The addition of cholesterol reduces the orientational disorder and inhibits the formation of the isotropic phase. These correlate well with the antimicrobial activities of PG-1.

The nature of the narrow peak at 1.5 ppm in the POPC/POPG spectrum is better understood from the analysis of the ^{31}P spectra. One-dimensional ^{31}P spectra of 0° and 90° aligned samples indicate that the 1.5 ppm peak indeed does not have any residual anisotropy. 2D ^{31}P exchange spectra further show that the isotropic domain is spatially well separated from the oriented bilayers, since even after a mixing time of 400 ms the cross-peak between the 0° peak and the isotropic peak is weak. These observations rule out the presence of toroidal pores in the equilibrium state of the membrane, since pore-lining lipids must undergo anisotropic motion and should, by definition, be spatially close to the oriented lipids. We believe the isotropic peak most likely corresponds to small lipid vesicles that originated from the bilayer but have fragmented from it. The lipids in these vesicles undergo isotropic motions on time scales slightly faster than the inverse of the ^{31}P CSA, since the ^{31}P peak width of 1.6 kHz is broader than the extreme narrowing limit. This isotropic motion can be overall tumbling of the vesicles or lateral diffusion of the lipid molecules on the vesicle surface. In fact, the broad POPC peak between −15 and 20 ppm (Figure 1c) may already signal an incipient isotropic domain, which is, however, not sufficiently mobile to be distinguished from the unoriented lipids. The lack of exchange between the lamellar and nonlamellar phases has also been detected in lipid membranes without any peptides (*40*). This suggests that the spatial separation of lamellar and nonlamellar lipids, whatever the origin, may be general. From the ^{31}P spectra alone, we cannot firmly exclude the more complex cubic phases as the origin of the isotropic peak. Such cubic-phase lipids have been observed to form in gramicidin S (GS) using X-ray diffraction (*27*, *28*) and in equinatoxin II using electron microscopy. However, given the relatively broad line width of the isotropic peak (∼10 ppm) in the PG-1-containing POPC/POPG spectrum, which is likely dynamic in origin, we favor the vesicle/micelle hypothesis.

The ^{31}P-detected ^{1}H spin diffusion spectra (Figure 8) indicate that the peptide is distributed in both the residual oriented bilayer and the isotropic domain to allow ^{1}H spin diffusion to reduce the ^{31}P signals of both morphologies by similar extents. It is difficult to quantify the relative amounts of the peptide bound to the bilayer versus the isotropic domain, since the ^{1}H spin diffusion coefficients are likely to be very different between the two domains. If the isotropic domain, despite its low rate of diffusion due to motion, had shown a preferential decrease of the ^{31}P intensity, then it would unambiguously signify the predominant association of the peptide with the isotropic phase. The fact that the 0° and the isotropic peaks dephase similarly implies that PG-1 may partition slightly more into the isotropic phase than to the residual oriented bilayer. Overall, it is clear that PG-1 is *not* exclusively bound to the isotropic vesicles but is also associated with the residual lamellar bilayer.

It is useful to compare the interaction of PG-1 with lipids to those of other membrane-active peptides. A number of peptides such as GS (*9*, *41*), equinatoxin II (*28*, *42*), and melittin (*28*) have been found to cause the formation of isotropic phases. However, for the relatively nonspecific antimicrobial peptides and for hemolytic peptides, the isotropic phase is usually not correlated with the presence of anionic lipids. For example, GS creates isotropic phases in bilayers of neutral sphingomyelin and phosphatidylethanolamine as well as in bilayers of anionic phosphatidylglycerol and phosphatidylserine (*9*). For the cholesterol-binding toxins equinatoxin II and pneumolysin, which target mammalian cells, isotropic lipids are formed only in the presence of sphingomyelin (*28*, *42*) and cholesterol (*43*). In contrast, the selective antimicrobial peptides nisin and mastoparan resemble PG-1 in that they form nonlamellar isotropic phases only in anionic membranes (*44*, *45*).

The observed protecting effect of cholesterol against PG-1's disruption of the membrane also resembles the behavior of several other antimicrobial peptides. ^{31}P NMR showed that cholesterol inhibits the formation of isotropic lipids by nisin (*45*) and to a lesser extent by GS (*46*). For magainin 2, a 4-fold increase in the peptide amount is required to cause 50% liposome lysis in the presence of cholesterol versus in its absence (*7*). These studies suggest that there is a good correlation between the function of membrane peptides (antimicrobial or cytotoxic) and the formation of nonlamellar phases in the target membranes of suitable composition (anionic or cholesterol-containing).

We hypothesize that the cationic and amphipathic nature of the PG-1 β-sheet is the main cause for its membrane selectivity. The cationic Arg residues facilitate the binding of PG-1 to anionic POPC/POPG membranes, while the hydrophobic patch favors insertion of PG-1 into the membrane. Once tightly bound, PG-1 apparently induces a strong positive curvature strain to the bilayer, eventually leading to the formation of isotropic vesicles. No such isotropic vesicles are seen in zwitterionic POPC bilayers, even though a significant amount of static disorder is seen. This may reflect weaker binding of the peptide to the zwitterionic membrane and thus less positive curvature strain. Cholesterol's protecting effect may result from the fact that its is embedded in the hydrophobic part of the membrane and thus counteracts the positive curvature strain. Studies of the structure−activity relationships of PG-1 and its analogues indicate that the antimicrobial activities of PG-1 decrease when the number of cationic residues is reduced and when the hydrophobic residues are replaced with polar amino acids (*16*). The importance of the amphipathic structure to membrane disruption is also supported by the comparison with the cyclic β-sheet peptide, RTD-1, which does not contain a hydrophobic patch. Solid-state NMR studies indicate that RTD-1 does not promote an isotropic phase in the anionic membrane and cholesterol also plays a less beneficial role (*47*).

The ^{13}C T_2 relaxation times of POPC segments in the POPC/POPG and POPC/Chol membranes provide further insights into the heterogeneity of the membrane mixtures. Regardless of whether the membranes are bound to PG-1,

the T_2 values measured from CP are shorter than those from the DP experiment, indicating the presence of dynamic heterogeneity in the mixed membranes. In the absence of PG-1, the core of the POPC molecule in the POPC/POPG bilayer shows T_2 ratios close to 1 while the ends of the molecule have more different T_2 values. This indicates that the hydrophobic part of the membrane is more homogeneous than the interfacial region, as expected for the identical chain but differing headgroup mixture. For the POPC/Chol membrane, the dynamic heterogeneity is far more pronounced (Figure 10) and is present across the entire depth of the membrane. This is consistent with the complexity of the cholesterol/phospholipid phase diagrams and the existence of liquid-ordered and liquid-disordered phases with suitable temperatures and compositions (*34*, *35*). The $T_{2,DP}$ values of the POPC acyl chains are significantly lower in the POPC/Chol membrane than in the POPC/POPG membrane. This is consistent with the fact that cholesterol is incorporated into the hydrophobic core of the bilayer and increases the chain rigidity (*36*, *48*, *49*).

PG-1 binding decreases the T_2 ratios of the POPC/POPG membrane but increases the T_2 ratios of the POPC/Chol membrane. The former indicates that the POPC/POPG membrane became more heterogeneous upon PG-1 binding. In light of the oriented-membrane results, this enhanced heterogeneity can be attributed to the formation of the isotropic phase, where motions slower than the uniaxial rotation of the lipids and comparable to the time scale of the ^{31}P CSA are present. These slow motions dephase the ^{13}C signals during the Hahn echo delay, thus yielding shorter T_2 values. In contrast, the already heterogeneous POPC/Chol membrane becomes less heterogeneous upon PG-1 binding. We hypothesize that PG-1 preferentially binds to the POPC-rich domain, triggering slower motions that are similar to those of POPC molecules in the cholesterol-rich domain. We have previously measured the differential ^{13}C T_2 relaxation times of DLPC bilayers with bound PG-1 (*22*). The $T_{2,CP}$/$T_{2,DP}$ ratios of the DLPC carbons in the presence of PG-1 are closer to 1 than those of the mixed membranes studied here. This indicates that the DLPC/PG-1 membrane is more homogeneous than the anionic and cholesterol-containing membranes.

In conclusion, ^{31}P, ^{2}H, and ^{13}C NMR of oriented and unoriented membranes with different compositions show that PG-1 fragments anionic membranes into isotropic vesicles while causing largely static disorder in the zwitterionic POPC bilayer. The addition of cholesterol attenuates the orientational disorder of the membrane and suppresses the formation of the isotropic phase. Once the anionic isotropic vesicles are formed, PG-1 is not exclusively bound to the nonlamellar phase but is also present in the residual oriented bilayers. The presence of the isotropic phase increases the dynamic heterogeneity of the anionic membrane, while the POPC/Chol membrane appears to be partially homogenized by PG-1.

REFERENCES

1. Epand, R. M., and Vogel, H. J. (1999) Diversity of antimicrobial peptides and their mechanisms of action, *Biochim. Biophys. Acta 1462*, 11−28.
2. Hancock, R. E., and Chapple, D. S. (1999) Peptide antibiotics, *Antimicrob. Agents Chemother. 43*, 1317−1323.
3. Ratledge, C., and Wilkinson, S. G. (1988) *Microbial Lipids*, Academic Press, London.
4. Blagovic, B., Rupcic, J., Mesaric, M., Georgiu, K., and Maric, V. (2001) Lipid composition of Brewer's yeast, *Food Technol. Biotechnol. 39*, 175−181.
5. Gennis, R. B. (1989) *Biomembranes: Molecular Structure and Function*, Springer, New York.
6. Yeagle, P. L. (1988) *The Biology of Cholesterol*, pp 121−146, CRC Press, Boca Raton, FL.
7. Matsuzaki, K., Sugishita, K., Fujii, N., and Miyajima, K. (1995) Molecular basis for membrane selectivity of an antimicrobial peptide, magainin 2, *Biochemistry 34*, 3423−3429.
8. Matsuzaki, K., Harada, M., Handa, T., Funakoshi, S., Fujii, N., Yajima, H., and Miyajima, K. (1989) Magainin 1-induced leakage of entrapped calcein out of negatively-charged lipid vesicles, *Biochim. Biophys. Acta 981*, 130−134.
9. Prenner, E. J., Lewis, R. N., and McElhaney, R. N. (1999) The interaction of the antimicrobial peptide gramicidin S with lipid bilayer model and biological membranes, *Biochim. Biophys. Acta 1462*, 201−221.
10. Matsuzaki, K. (1999) Why and how are peptide-lipid interactions utilized for self-defense? Magainins and tachyplesins as archetypes, *Biochim. Biophys. Acta 1462*, 1−10.
11. Gazit, E., Lee, W. J., Brey, P. T., and Shai, Y. (1994) Mode of action of the antibacterial cecropin B2: a spectrofluorometric study, *Biochemistry 33*, 10681−10692.
12. Kokryakov, V. N., Harwig, S. S., Panyutich, E. A., Shevchenko, A. A., Aleshina, G. M., Shamova, O. V., Korneva, H. A., and Lehrer, R. I. (1993) Protegrins: leukocyte antimicrobial peptides that combine features of corticostatic defensins and tachyplesins, *FEBS Lett. 327*, 231−236.
13. Aumelas, A., Mangoni, M., Roumestand, C., Chiche, L., Despaux, E., Grassy, G., Calas, B., and Chavanieu, A. (1996) Synthesis and solution structure of the antimicrobial peptide protegrin-1, *Eur. J. Biochem. 237*, 575−583.
14. Fahrner, R. L., Dieckmann, T., Harwig, S. S., Lehrer, R. I., Eisenberg, D., and Feigon, J. (1996) Solution structure of protegrin-1, a broad-spectrum antimicrobial peptide from porcine leukocytes, *Chem. Biol. 3*, 543−550.
15. Harwig, S. S., Waring, A., Yang, H. J., Cho, Y., Tan, L., and Lehrer, R. I. (1996) Intramolecular disulfide bonds enhance the antimicrobial and lytic activities of protegrins at physiological sodium chloride concentrations, *Eur. J. Biochem. 240*, 352−357.
16. Chen, J., Falla, T. J., Liu, H., Hurst, M. A., Fujii, C. A., Mosca, D. A., Embree, J. R., Loury, D. J., Radel, P. A., Cheng Chang, C., Gu, L., and Fiddes, J. C. (2000) Development of protegrins for the treatment and prevention of oral mucositis: structure−activity relationships of synthetic protegrin analogues, *Biopolymers 55*, 88−98.
17. Steinberg, D. A., Hurst, M. A., Fujii, C. A., Kung, A. H. C., Ho, J. F., Cheng, F. C., Loury, D. J., and Fiddes, J. C. (1997) Protegrin-1: a broad-spectrum, rapidly microbicidal peptide with in vivo activity, *Antimicrob. Agents Chemother. 41*, 1738−1742.
18. Tam, J. P., Wu, C., and Yang, J. L. (2000) Membranolytic selectivity of cystine-stabilized cyclic protegrins, *Eur. J. Biochem. 267*, 3289−3300.
19. Tamamura, H., Murakami, T., Horiuchi, S., Sugihara, K., Otaka, A., Takada, W., Ibuka, T., Waki, M., Yamamoto, N., and Fujii, N. (1995) Synthesis of protegrin-related peptides and their antibacterial and anti-human immunodeficiency virus activity, *Chem. Pharm. Bull. 43*, 853−858.
20. Yamaguchi, S., Waring, A., Hong, T., Lehrer, R., and Hong, M. (2002) Solid-State NMR Investigations of Peptide-Lipid Interaction and Orientation of a β-Sheet Antimicrobial Peptide, Protegrin, *Biochemistry 41*, 9852−9862.
21. Buffy, J. J., Waring, A. J., Lehrer, R. I., and Hong, M. (2003) Immobilization and Aggregation of the Antimicrobial Peptide Protegrin-1 in Lipid Bilayers Investigated by Solid-State NMR, *Biochemistry 42*, 13725−13734.
22. Buffy, J. J., Hong, T., Yamaguchi, S., Waring, A., Lehrer, R. I., and Hong, M. (2003) Solid-State NMR Investigation of the Depth of Insertion of Protegin-1 in Lipid Bilayers Using Paramagnetic Mn^{2+}, *Biophys. J. 85*, 2363−2373.
23. Hallock, K. J., Henzler Wildman, K., Lee, D. K., and Ramamoorthy, A. (2002) An innovative procedure using a sublimable solid to align lipid bilayers for solid-state NMR studies, *Biophys. J. 82*, 2499−2503.

24. Glaser, R. W., and Ulrich, A. S. (2003) Susceptibility corrections in solid-state NMR experiments with oriented membrane samples. Part I: applications, *J. Magn. Reson. 164*, 104−114.
25. Bodenhausen, G., Freeman, R., and Turner, D. L. (1977) Suppresion of artifacts in two-dimensional J spectroscopy, *J. Magn. Reson. 27*, 511−514.
26. Huster, D., Yao, X. L., and Hong, M. (2002) Membrane Protein Topology Probed by ^{1}H Spin Diffusion from Lipids Using Solid-State NMR Spectroscopy, *J. Am. Chem. Soc. 124*, 874−883.
27. Epand, R. M. (1998) Lipid polymorphism and protein−lipid interactions, *Biochim. Biophys. Acta 1376*, 353−368.
28. Anderluh, G., Serra, M. D., Viero, G., Guella, G., Macek, P., and Menestrina, G. (2003) Pore formation by equinatoxin II, a eukaryotic protein toxin, occurs by induction of nonlamellar lipid structures, *J. Biol. Chem. 278*, 45216−45223.
29. Yamaguchi, S., Huster, D., Waring, A., Lehrer, R. I., Tack, B. F., Kearney, W., and Hong, M. (2001) Orientation and Dynamics of an Antimicrobial Peptide in the Lipid Bilayer by Solid-State NMR, *Biophys. J. 81*, 2203−2214.
30. Seelig, A., and Seelig, J. (1974) Dynamic structure of fatty acyl chains in phospholipid bilayers by ^{2}H NMR, *Biochemistry 13*, 4839.
31. Huster, D., Yao, X., Jakes, K., and Hong, M. (2002) Conformational changes of colicin Ia channel-forming domain upon membrane binding: a solid-state NMR study, *Biochim. Biophys. Acta 1561*, 159−170.
32. Fenske, D. B., and Jarrell, H. C. (1991) Phosphorous-31 two-dimensional solid-state exchange NMR, *Biophys. J. 59*, 55−69.
33. Picard, F., Paquet, M.-J., Dufourc, E. J., and Auger, M. (1998) Measurement of the lateral diffusion of dipalmitoylphosphatidylcholine adsorbed on silica beads in the absence and presence of melittin: A ^{31}P two-dimensional exchange solid-state NMR study, *Biophys. J. 74*, 857−868.
34. McConnell, H. M., and Vrljic, M. (2003) Liquid−liquid immiscibility in membranes, *Annu. Rev. Biophys. Biomol. Struct. 32*, 469−492.
35. Sankaram, M. B., and Thompson, T. E. (1990) Interaction of cholesterol with various glycerophospholipids and sphingomyelin, *Biochemistry 29*, 10670−10675.
36. Sankaram, M. B., and Thompson, T. E. (1990) Modulation of phospholipid acyl chain order by cholesterol. A solid-state ^{2}H nuclear magnetic resonance study, *Biochemistry 29*, 10676−10684.
37. Hancock, R. E., and Scott, M. G. (2000) The role of antimicrobial peptides in animal defenses, *Proc. Natl. Acad. Sci. U.S.A. 97*, 8856−8861.
38. Papo, N., and Shai, T. (2003) Can we predict biological activity of antimicrobial peptides from their interactions with model phospholipid membranes? *Peptides 24*, 1693−1703.
39. Blondelle, S. E., Lohner, K., and Aguilar, M. (1999) Lipid-induced conformation and lipid-binding properties of cytolytic and antimicrobial peptides: determination and biological specificity, *Biochim. Biophys. Acta 1462*, 89−108.
40. Fenske, D. B., and Cullis, P. R. (1992) Chemical exchange between lamellar and nonlamellar lipid phases. A one- and two-dimensional ^{31}P NMR study, *Biochim. Biophys. Acta 1108*, 201−209.
41. Prenner, E. J., Lewis, R. N. A. H., Neuman, K. C., Gruner, S. M., Kondejewski, L. H., Hodges, R. S., and McElhaney, R. N. (1997) Nonlamellar phases induced by the interaction of gramicidin S with lipid bilayers. A possible relationship to membrane-disrupting activity, *Biochemistry 36*, 7906−7916.
42. Bonev, B. B., Lam, Y. H., Anderluh, G., Watts, A., Norton, R. S., and Separovic, F. (2003) Effects of the eukaryotic pore-forming cytolysin equinatoxin II on lipid membranes and the role of sphingomyelin, *Biophys. J. 84*, 2382−2392.
43. Bonev, B. B., Gilbert, R. J., Andrew, P. W., Byron, O., and Watts, A. (2001) Structural analysis of the protein/lipid complexes associated with pore formation by the bacterial toxin pneumolysin, *J. Biol. Chem. 276*, 5714−5719.
44. Hori, Y., Demura, M., Niidome, T., Aoyagi, H., and Asakura, T. (1999) Orientational behavior of phospholipid membranes with mastoparan studied by ^{31}P solid-state NMR, *FEBS Lett. 455*, 228−232.
45. Jastimi, R. E., Edwards, K., and Lafleur, M. (1999) Characterization of permeability and morphological perturbations induced by nisin on phosphatidylcholine membranes, *Biophys. J. 77*, 842−852.
46. Prenner, E. J., Lewis, R. N., Jelokhani-Niaraki, M., Hodges, R. S., and McElhaney, R. N. (2001) Cholesterol attenuates the interaction of the antimicrobial peptide gramicidin S with phospholipid bilayer membranes, *Biochim. Biophys. Acta 1510*, 83−92.
47. Buffy, J. J., McCormick, M. J., Wi, S., Waring, A. J., Lehrer, R. I., and Hong, M. (2004) Solid-State NMR Investigation of the Selective Perturbation of Lipid Bilayers by the Cyclic Antimicrobial Peptide RTD-1, *Biochemistry*, *43*, 9800−9812.
48. Villalain, J. (1996) Location of cholesterol in model membranes by magic-angle-sample-spinning NMR, *Eur. J. Biochem. 241*, 586−593.
49. Yeagle, P. L., Hutton, W. C., Huang, C., and Martin, R. B. (1977) Phospholipid head-group conformations: intermolecular interactions and cholesterol effects, *Biochemistry 16*, 4344−4349.
50. Sparling, M. L., Zidovetzki, R., Muller, L., and Chan, S. I. (1989) Analysis of membrane lipids by 500 MHz ^{1}H NMR, *Anal. Biochem. 178*, 67−76.
51. Forbes, J., Bowers, J., Shan, X., Moran, L., Oldfield, E., and Moscarello, M. A. (1988) Some new developments in solid-state nuclear magnetic resonance spectroscopic studies of lipids and biological membranes, including the effects of cholesterol in model and natural systems, *J. Chem. Soc., Faraday Trans. 1 84*, 3821−3849.

BI048650T